Supplement Experimental Procedures

RNA sequencing analysis
RNA-seq data sets detailed in Table S1 were aligned to ANP32A genomic DNA assemblies from their respective species. Gene indices were built using HISAT2 (function -build; -q -f) (Kim et al., 2015). Indices for *Aptenodytes forsteri* and *Sturnus vulgaris* were insufficient for initial alignment. These regions were re-built using a custom Python script (available upon request) to search RNA-seq files for reads mapping proximal to gene regions with poor alignment and using these to complete the gene assembly. Genomic DNA sequence was unavailable for *Leucophaeus atricilla,* so reads were aligned to *Calidris Pugnax* and as above, iteratively corrected to achieve alignment. RNA-seq datasets were first quality assessed using fastqc (Andrews, 2010), trimmed with bbduk (parameters ktrim=r, k=21, mink=10, hdist=1) (Bushnell, 2015), and aligned using hisat2 (option -U -S). Splicing events were visualized in IGV (sashimi plot function) to enumerate the intron-spanning reads between avian exons 4, 5, and 6 (Katz et al., 2015).

Cells, viruses and plasmids
Mammalian 293T, A549, MDBK and MDCK cells were grown in DMEM supplemented with 10% FBS. Chicken LMH cells were grown in DMEM/F-12 with 5% FBS. All cells were maintained at 37 °C, 5% CO_2. Cell stocks were routinely tested for mycoplasma (MycoAlert, Lonza).

Viruses and plasmid clones were derived from A/WSN/33 (H1N1; WSN) and A/green-winged teal/Ohio/175/1986 (H2N1; S009) (Mehle and Doudna, 2008, 2009). Recombinant virus was rescued by transfecting co-cultures of 293T and MDCK cells with pTMΔRNP (encoding WSN vRNA segments HA, NA, M, and NS), the bi-directional pBD plasmids (encoding vRNA and mRNA) PB1, PA, NP, and the indicated *PB2* mutants (Mehle and Doudna, 2008; Neumann et al., 2005). S009 WT and SRK viruses contain NP and polymerase genes from S009 and the remaining segments from WSN (Mehle and Doudna, 2009). WSN PB2-FLAG-143 virus (hereafter referred to as WSN PB2-FLAG) was generated as previously described (Kirui et al., 2016; Dos Santos Afonso et al., 2005). WSN PB2-K627E-FLAG virus was generated similarly. Viral stocks were amplified on MDBK cells and titrated by plaque assay on MDCK cells. Influenza virus infections were performed by inoculating cells with stocks diluted in virus growth media (VGM): DMEM supplemented with penicillin/streptomycin, 25 mM HEPES, 0.3% BSA, and 0.25 – 0.5 µg/ml TPCK-trypsin. Multi-cycle growth curves were performed by inoculating A549 cells at a multiplicity of infection (MOI) of 0.1 at 33 °C, collecting supernatants at the indicated times postinfection, and titering samples by plaque assay on MDCK cells.

Gallus gallus ANP32A encoding a 29 amino acid insert (XM_004943928, chANP32A$_{29}$) was codon-optimized, synthesized (IDT, Inc.) and cloned into pENTR-D/TEV TOPO without a stop codon (Invitrogen). This construct was used as a template for inverse PCR to create chANP32A encoding a 33 amino acid insert (XM_413932, chANP32A$_{33}$). pDONR221-ANP32A encoding human *ANP32A* (huANP32A) was acquired from the DNASU Plasmid Repository (HsCD00042415). PCR was used to insert the 29 amino acid *Gallus* repeat into the human gene to create pDONR221-huANP32A$_{+29}$, to remove the repeat from the *Gallus* construct to create pENTR- chANP32A$_{\Delta}$, and to introduce a stop codon for generation of untagged ANP32A vectors. Coding sequences for the WSN PB2 627 domain (amino acids 538-676) or the 627 domain plus the NLS (amino acids 538-759) were cloned into pENTR-D/TEV TOPO. V5-tagged expression constructs for cell culture were created by Gateway recombination (Invitrogen) into pCDNA6.2 and pLX304 (Addgene 25890). Bacterial expression constructs were created by recombination into pHGGWA and pHMGWA (Busso et al., 2005). Influenza virus reporter gene and micro gene constructs were previously described (Kirui et al., 2016).

VSV-G pseudotyped lentivirus was prepared by transfecting 293T cells with pLX304, psPAX2 and pMD2.G. Resultant viruses were used to transduce A549 cells. Cells were selected with blasticidin to obtain lines stably expressing ANP32A.

Polymerase activity assays
RNP complexes were reconstituted by co-transfecting cells with p3X-1T to express PB2, PB1-TAP, and PA, pCDNA6.2 NP-V5 to express NP, and human or chicken pol I-driven vNA-Luc reporters (Mehle and Doudna, 2008). The G3A, C8U (3-8) mutant in the 3' vRNA UTR was previously described (Neumann and Hobom, 1995) and incorporated into a vNA-Luc reporter by PCR mutagenesis. pRL-SV40 (Promega) constitutively expressing Renilla luciferase was included as a control to normalize gene expression. Cells were lysed one day post-transfection, luciferase activities were measured, and firefly luciferase was normalized to the internal Renilla control. Protein levels in lysate were evaluated by Western blotting using anti-V5-HRP (Sigma, 1:10,000) to simultaneously detect PB1-TAP, NP-V5 and ANP32A-V5.

Co-immunoprecipitations
Plasmids expressing PB1, PA, PB2-FLAG (WT or K627E) and ANP32A-V5 were co-transfected into 293T cells. The catalytically inactive PB1a (D445A/D446A) mutant was created by PCR as previously described (Vreede et al., 2004). To test the effect of viral RNA on polymerase:ANP32A interactions, plasmids expressing vNA-Luc or cNA-Luc reporters were included when indicated. Cells were lysed two days post-transfection in co-immunoprecipitation (co-IP) buffer (50 mM Tris, pH7.5; 150 mM NaCl; 0.5% NP40) and clarified by centrifugation. Lysates were pre-cleared with protein A agarose

(Santa Cruz) for 1 h followed by affinity capture with anti-FLAG agarose resin (M2, Sigma) overnight. Immunoprecipitates were recovered, washed four times with co-IP buffer and eluted by boiling in Laemmli sample buffer. Immunoprecipitates and input samples were separated by SDS-PAGE, semi-dry transferred to PVDF membranes in Bjerrum Schafer-Nielsen buffer, and probed for ANP32A with anti-V5 HRP (Sigma) or PB2 with rabbit polyclonal anti-PB2 (Mehle and Doudna, 2008). Chemiluminescent images were captured on an Odyssey Fc Imager and quantified using Image Studio v5.2.5 (LI-COR).

RNP assembly in the presence or absence of ANP32A was measured as previously described (Mondal et al., 2015). To test protein interactions during infection, wild-type A549 cells or those stably expressing ANP32A were inoculated with WSN PB2-FLAG or PB2-K627E-FLAG (MOI 0.2). Cells were lysed 18-24 hpi and immunoprecipitations were performed as above. NP was detected by western blot with anti-RNP antibody (BEI NR-3133).

Purification and *in vitro* interactions of recombinant protein

Rosetta 2(DE3)pLysS *E. coli* were transformed with pHMGWA-ANP32A or pHGGWA-PB2 constructs, grown to OD 0.8 and induced with 0.5 mM IPTG at 16 °C for 18-20 h. HisMBP-ANP32A proteins were purified as previously described and dialyzed into 50 mM HEPES pH 7.9, 150 mM KCl, 1 mM DTT and 10% glycerol (Sugiyama et al., 2015). HisGST-PB2 proteins were purified as before and dialyzed into 10 mM Tris-HCl pH 7.0, 200 mM NaCl, 10% glycerol (Tarendeau et al., 2008). *In vitro* protein interactions were performed by mixing 20 µg each of bait and prey proteins in 100 µl total interaction buffer (10 mM HEPES pH 7.5, 100 mM KCl, 10 mM NaCl, 5 mM $MgCl_2$) followed by rotating for 1 h at room temperature (Habrukowich et al., 2010). Bait proteins were then captured with 10 µl MagneGST glutathione particles (Promega). Pull-down complexes were washed four times with interaction buffer, eluted by boiling in Laemmli sample buffer, separated by SDS-PAGE and detected by Coomassie staining. Input lanes contain 5 µg protein.

Primer extension

NP-independent transcription and replication of a micro-gene vRNA template (77 nt derived from *NP* gene segment) was performed in transfected 293T cells (Kirui et al., 2016; Turrell et al., 2013). Total RNA was isolated from cells two days post-transfection using TRIzol (Invitrogen) and the levels of mRNA and vRNA were quantified by primer extension (Fodor and Smith, 2004; Mehle and Doudna, 2008). Primers that recognize NP77 in the plus sense (5'-TGATTTCGATGTCACTCTGTGAGT-3') or minus sense (5'-GCAGGGTAGATAATCACTGACAGAG-3') or 5s ribosomal RNA (5'-ACCCTGCTTAGCTTCCGAGA-3') were radio-labeled and used in the reaction. These primers are expected to generate products indicative of mRNA (approximately 56-60 nt), vRNA (70 nt) and 5s RNA (62 nt). Products were resolved by denaturing PAGE (12% acrylamide, 7 M urea, 0.5x TBE), dried and detected by phosphorimaging.

Andrews, S. (2010). FastQC: A quality control tool for high throughput sequence data. Available at http://www.Bioinformatics.Babraham.Ac.Uk/Projects/Fastqc/.

Bushnell, B. (2015). BBMap (version 37.75) [Software]. Available at Https://sourceforge.net/projects/bbmap/.

Busso, D., Delagoutte-Busso, B., and Moras, D. (2005). Construction of a set Gateway-based destination vectors for high-throughput cloning and expression screening in Escherichia coli. Anal. Biochem. *343*, 313–321.

Fodor, E., and Smith, M. (2004). The PA Subunit Is Required for Efficient Nuclear Accumulation of the PB1 Subunit of the Influenza A Virus RNA Polymerase Complex The PA Subunit Is Required for Efficient Nuclear Accumulation of the PB1 Subunit of the Influenza A Virus RNA Polymerase Compl. Society *78*, 9144–9153.

Habrukowich, C., Han, D.K., Le, A., Rezaul, K., Pan, W., Ghosh, M., Li, Z., Dodge-Kafka, K., Jiang, X., Bittman, R., et al. (2010). Sphingosine interaction with acidic leucine-rich nuclear phosphoprotein-32A (ANP32A) regulates PP2A activity and cyclooxygenase (COX)-2 expression in human endothelial cells. J. Biol. Chem. *285*, 26825–26831.

Katz, Y., Wang, E.T., Silterra, J., Schwartz, S., Wong, B., Thorvaldsdóttir, H., Robinson, J.T., Mesirov, J.P., Airoldi, E.M., and Burge, C.B. (2015). Quantitative visualization of alternative exon expression from RNA-seq data. Bioinformatics *31*, 2400–2402.

Kim, D., Langmead, B., and Salzberg, S.L. (2015). HISAT: A fast spliced aligner with low memory requirements. Nat. Methods *12*, 357–360.

Kirui, J., Mondal, A., and Mehle, A. (2016). Ubiquitination Upregulates Influenza Virus Polymerase Function. J. Virol. *90*, 10906–10914.

Mehle, A., and Doudna, J.A. (2008). An Inhibitory Activity in Human Cells Restricts the Function of an Avian-like Influenza Virus Polymerase. Cell Host Microbe *4*, 111–122.

Mehle, A., and Doudna, J. a (2009). Adaptive strategies of the influenza virus polymerase for replication in humans. Proc. Natl. Acad. Sci. U. S. A. *106*, 21312–21316.

Mondal, A., Potts, G.K., Dawson, A.R., Coon, J.J., and Mehle, A. (2015). Phosphorylation at the homotypic interface regulates nucleoprotein oligomerization and assembly of the influenza virus replication machinery. PLoS Pathog. *11*, e1004826.

Neumann, G., and Hobom, G. (1995). Mutational analysis of influenza virus promoter elements in vivo. J Gen Virol *76 (Pt 7)*, 1709–1717.

Neumann, G., Fujii, K., Kino, Y., and Kawaoka, Y. (2005). An improved reverse genetics system for influenza A virus

generation and its implications for vaccine production. Proc. Natl. Acad. Sci. U. S. A. *102*, 16825–16829.
Dos Santos Afonso, E., Escriou, N., Leclercq, I., Van Der Werf, S., and Naffakh, N. (2005). The generation of recombinant influenza A viruses expressing a PB2 fusion protein requires the conservation of a packaging signal overlapping the coding and noncoding regions at the 5??? end of the PB2 segment. Virology *341*, 34–46.
Sugiyama, K., Kawaguchi, A., Okuwaki, M., and Nagata, K. (2015). PP32 and APRIL are host cell-derived regulators of influenza virus RNA synthesis from cRNA. Elife *4*, e08939.
Tarendeau, F., Crepin, T., Guilligay, D., Ruigrok, R.W.H., Cusack, S., and Hart, D.J. (2008). Host determinant residue lysine 627 lies on the surface of a discrete, folded domain of influenza virus polymerase PB2 subunit. PLoS Pathog. *4*.
Turrell, L., Lyall, J.W., Tiley, L.S., Fodor, E., and Vreede, F.T. (2013). The role and assembly mechanism of nucleoprotein in influenza A virus ribonucleoprotein complexes. Nat. Commun. *4*, 1591.
Vreede, F.T., Jung, T.E., and Brownlee, G.G. (2004). Model suggesting that replication of influenza virus is regulated by stabilization of replicative intermediates. J. Virol. *78*, 9568–9572.

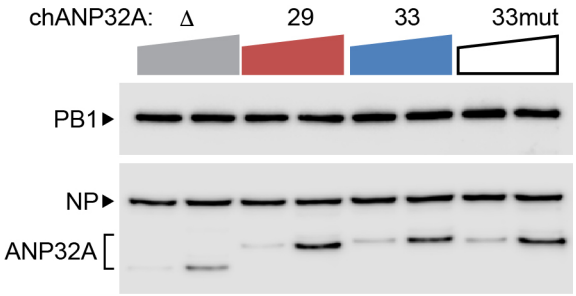

Supplemental Figure 1: ANP32A variants are expressed at similar levels (Associated with Fig. 2D). Samples from Fig 2D containing the two highest amounts of each ANP32A variant were re-run on the same gel to enable comparison. Proteins were detected by western blot